PHYSICAL REVIEW B VOLUME 14, NUMBER 8 15 OCTOBER 1976

Application of the linear combination of muffin-tin orbitals energy-band method to surfaces and molecules

R. V. Kasowski
Central Research and Development Department, E. I. du Pont de Nemours and Company, Wilmington, Delaware 19898
(Received 1 March 1976)

The linear combination of muffin-tin orbitals method has been used to calculate the electronic properties of thin films of transition metals. A detailed discussion of these calculations is presented. We have also applied the method to calculate the energy levels of a single N_2 molecule. Finally, we show that the muffin-tin orbital basis set can be augmented with either Slater-type or Gaussian-type orbitals to facilitate more accurate molecular calculations.

I. INTRODUCTION

Recently, much attention has been devoted to the related problems of calculating the electronic states of transition-metal surfaces and the energy of atoms and molecules adsorbed onto these surfaces. An accurate description of electronic energy states would be valuable in unraveling some of the mystery surrounding the role of transition metals in catalysis. However, such calculations are difficult to perform because lattice periodicity, which is so helpful in three dimensions, is lost normal to the surface. New theoretical approaches must be devised to treat the semi-infinite solid.

One approach is to perform *ab initio* calculations of the electronic states of a semi-infinite film of finite thickness.[1-3] Such a model has great flexibility in that clean surfaces, reconstructed surfaces, and surfaces with chemisorbed atoms or molecules can be studied.

However, a serious complication in studying thin films is that the unit cell extends across the entire thickness of the film and thus contains at least as many atoms as there are layers. A particular surface structure such as $c(2\times 2)$ will double the number of atoms in the substrate part of the film's unit cell. The linear combination of muffin-tin orbitals (LCMTO) method[4,5] will be shown to be ideal for thin-film studies since large unit cells can be treated easily and the muffin-tin orbitals (MTO) can be chosen to satisfy proper boundary conditions.

The first *ab initio* thin-film calculations were performed by Alldredge and Kleinman for Li(001).[1] Their method utilized the pseudopotential approach and is limited to *sp* bonded systems not transition metals. Kleinman and Caruthers[6] have recently supplemented their plane-wave basis set with localized numerical functions so that it is applicable to *d*-band materials. Their results for Fe agree qualitatively with those of Kasowski[7] for W and Mo whose band structure is similar to that of Fe. They have not yet demonstrated that their revised method can be used to calculate the effects of surface relaxation[7] and atomic chemisorption[2] as Kasowski has already demonstrated with the LCMTO method. The only other thin-film method is that of Schluter and co-workers.[3] It is similar to the Alldredge and Kleinman[1] approach except that they use a basis set of traveling plane waves instead of standing waves; they impose periodic boundary conditions in the direction normal to the film surface, which is equivalent to the construction of a hypothetical solid composed of a periodic array of thin films, each separated by an open interval of several interatomic distances from the neighboring film.

In Sec. II, we describe the LCMTO method as applied to bulk crystals and discuss the modifications that are necessary to apply the technique to thin films. We also show how the basis set can be improved considerably by using the hypothetical solid of thin films devised by Cohen (see Ref. 3). In Sec. III, a prescription for constructing potentials for films is described. In Sec. IV we compare the results of localized basis MTO functions as compared to long-range MTO basis functions. We also show how the calculated surface properties are effected by the film thickness.

In Sec. V, we treat the nitrogen molecule, the purpose of which is to demonstrate that the LCMTO method is applicable to covalently bonded molecules as well. Nitrogen was selected because the ordering of the energy levels is well characterized experimentally and because several other theoretical calculations that have been carried out may be used to compare with the method presented here.

II. LCMTO THEORY

Before describing the thin-film LCMTO formalism, we will briefly review the general theory of the LCMTO method.[4,5] The potential, formed by

overlapping atomic charge densities, is expanded in spherical harmonics within (nonoverlapping) atomic Wigner-Seitz (AWS) cells. (For surfaces, the empty-space region is also expanded in AWS cells using empty lattice sites as cell centers.) Solutions, $\phi_{lm}(E,r)$, of the Schrödinger equation for the muffin-tin part of the potential are then used to construct muffin-tin orbitals (MTO's):

$$\chi_{lm}(E,\kappa,r)=\begin{cases}\phi_{lm}(E,\vec{r})+C_l(E,\kappa)\,\tilde{J}_{lm}(\kappa,\vec{r}), & r\le S\\ -S_l(E,\kappa)\,\tilde{K}_{lm}(\kappa,\vec{r}), & r\ge S.\end{cases}$$

C_l and S_l are determined by continuity of the logarithmic derivative at the muffin-tin sphere radius S. $\tilde{J}_{lm}(\kappa,\vec{r})$ is that solution, $J_{lm}(\kappa,\vec{r})$, of the wave equation which is orthogonalized to the core states of the potential at the origin, while $\tilde{K}_{lm}(\kappa,r)$ is a solution which is orthogonalized to the core states on all other sites. J_{lm} and K_{lm} are defined as products of spherical harmonics and spherical Bessel and Neumann functions such that they are regular at the origin and at infinity, respectively, and both are regular at $\kappa=0$.

We form a multicentered basis set of MTO's, i.e., the set of Bloch functions $\chi^{\vec{k}}_{lm}(E,\kappa^2)$ for fixed parameters E and κ^2, and apply the linear variational equation

$$\langle\chi^{\vec{k}}_{lm}(E,\kappa^2)\,|\,H-E\,|\,\chi^{\vec{k}}_{lm}(E,\kappa^2)\rangle=0, \qquad (1)$$

which is evaluated in Ref. 4. All multicentered integrals are eliminated by using summation theorems for spherical Bessel and Neumann functions. Actual evaluation of this equation has been discussed in detail in Ref. 4. The eigenvalues at the Γ point are plotted as a function of κ^2 in Fig. 1 for Si and Cu. The Cu levels are insensitive to κ^2, whereas κ^2 is a very important parameter in the basis set for Si. Consequently for Si, Eq. (1) must be evaluated at numerous energies E to obtain the best eigenvalues.

A significant simplification in the LCMTO method[5] is achieved by enlarging the basis set to include exponentially decaying MTO's and oscillating MTO's of fixed energies E_1 and E_2, respectively. The secular equation is now in the LCAO form

$$\langle\chi^{k}_{l_1m_1}(E_1,\kappa_1^2<0)+\chi^{k}_{l_2m_2}(E_2,\kappa_2^2>0)\,|\,H-E\,|\,\chi^{k}_{l_1m_1}(E_1,\kappa_1^2)+\chi^{k}_{l_2m_2}(E_2,\kappa_2^2)\rangle=0, \qquad (2)$$

with E_1 equal to some average of the low-energy valence states and E_2 equal to some average of the states near the Fermi surface. Equation (2) is computationally simpler than Eq. (1) even with the larger basis set because one obtains the one diagonalization of the secular equation all the eigenvalues at a particular $\vec{k}$ point [see Appendix A for evaluation of Eq. (2)]. Optimal values of the parameters are easily determined because the eigenvalues form broad minima as a function of E_1, κ_1^2, E_2, and κ_2^2. Furthermore, the broad minima indicate that it is no longer important to search for an optimal basis set. For Si, an optimal set for all k giving ~0.02-Ry accuracy with the more exact and costly method of Eq. (1) is $E_1=-3.2$ Ry, $\kappa_1^2=-0.25$ Ry, $E_2=-2.8$ Ry, and $\kappa_2^2=0.5$ Ry. This choice of κ_1^2 and κ_2^2 has also given energy bands in good agreement with photoemission measurements for[5] NiS and[8] MoS_2. E_1 and E_2 were adjusted to be in the energy range of the valence-band states.

Another advantage of Eq. (2) is that it is straightforward to obtain the distribution of a particular eigenstate among the atoms or AWS cells in the unit cell. The theorem[4]

$$K_L(r-Q)=\sum 4\pi C^{L}_{L'L''}\;J_{L'}(r)\;K^{*}_{L''}(Q), \qquad (3)$$

which is used to reduce multicenter integrals to single-center integrals, holds only for $|r|$ less than nearest-neighbor distance ($C^{L}_{L'L''}$ is the Clebsch-Gordan coefficient and $L=lm$). As a result all space must be divided into nonoverlapping atomic Wigner-Seitz cells. The normalization integral in Eq. (2) becomes

$$\sum_{\text{AWS}}(\psi_i\,|\,\psi_i)=1=\sum_{\text{AWS}}\rho_{\text{AWS}},$$

where ψ_i designates the ith eigenvector of energy E_i and the sum is performed over all AWS cells in the unit cell. ρ_{AWS} represents the probability

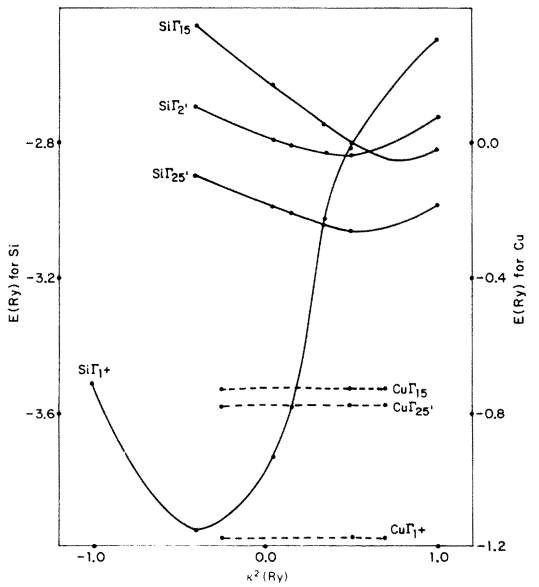

FIG. 1. Bulk eigenvalues at $\Gamma(0,0,0)$ for Si and Cu as a function of κ^2.

of finding the electron within site AWS. This will be very valuable especially for thin films where little ambiguity exists about how to divide the unit cell into AWS cells.

These considerations concerning choice of basis functions are directly applicable to the study of thin films. LCMTO equations for a single thin film are the same as in the bulk except that (i) the Bloch functions are two dimensional, and (ii) we must restrict κ^2 to being negative. The $\kappa^2 > 0$ MTO's are not normalizable in the free-space region for a single thin film. This does not present a problem for the study of most transition metals since from Fig. 1 the eigenvalues of Cu are well represented by MTO's that have $\kappa^2 < 0$. Similar results are obtained for Ni. However, the study of Si would require $\kappa^2 > 0$ MTO's.

The restriction on κ^2 can be overcome easily by treating a hypothetical solid consisting of thin films each separated by several angstroms from a neighboring film. Equation (2) is then applicable since $\kappa^2 > 0$ MTO's are normalizable for this geometry. One thus regains the full power and simplicity of the LCMTO approach. In Sec. IV we report successful application of this idea to Ni.

III. POTENTIAL

Potentials are constructed by overlapping atomic charge densities[9] and taking the cube root of the sum to approximate exchange and correlation. This potential has proved extremely successful in describing the electronic properties of the cubic and hexagonal close-packed transition metals.[10] We feel it should also be successful in describing the surface, a state intermediate between bulk and atom.

The first step is to expand all of space into nonoverlapping atomic Wigner-Seitz (AWS) cells such that the distance to the furthest corner of the cell is less than the nearest-neighbor distance.[4] For a thin film, we divide the region near the surface into AWS cells by choosing empty lattice sites as cell centers.

The potential is then expanded in spherical harmonics $[\sum V_L^{\mathrm{WS}}(r) Y_L(r)]$ within the AWS. We use $L = lm$ throughout this section. In order to reduce all integrals in Eq. (2) to radial integrals times a Clebsch-Gordan coefficient, the AWS potential $\sum Y_L V_L^{\mathrm{WS}}$ is again expanded in spherical harmonics $[\sum \bar{V}_L(r) Y_L(r)]$. A particular $\bar{V}_L(r) = \sum_{L'} f_{L'L} V_{L'}^{\mathrm{WS}}(r)$, where $f_{L'L} = \int_{\mathrm{WS}} Y_L Y_{L'} \, d\Omega_{\mathrm{WS}}$. The expansion in angular momentum is usually truncated at $l = 8$ and $l' = 8$. The potentials $V_{L'}^{\mathrm{WS}}(r)$ and coefficient $f_{L'L}(r)$ we obtained by Monte-Carlo sampling techniques.

The potential is formed by overlapping atomic charge density tails and Coulomb contributions of all neighbors out to convergence. Bulk potentials are constructed from a full set of nearest neighbors. A potential at the surface is different only in that one has fewer nearest neighbors over which to sum charge density and Coulomb tails. Thus all symmetrically inequivalent atoms in the film have different potentials.

It is also appropriate to define an abrupt termination potential. It is formed by placing a bulk potential at all AWS sites in the film including the surface layer. The potential is zero outside this surface layer and forms a corrugated surface. In Sec. IV we will show what magnitude of error results from such a drastic cutoff. Our abrupt termination potential differs from that used in low-energy-electron diffraction (LEED) calculations[11] which is planar and often called a Cambridge potential.

IV. SURFACE CALCULATIONS

A thin film or slab is a simple model designed specifically for the calculation of surface properties of solids. It is approximate in that the film is finite in the direction perpendicular to the film, whereas a real crystalline material can be thousands of layers thick. The value of this model is that *ab initio* calculations can be easily performed for a variety of surface conditions: clean, reconstructed, relaxed, chemisorption, etc. In this section we investigate several aspects of this thin-film model that greatly influence the accuracy of the results and guide its applicability. We also will indicate how to improve the basis set used previously[2] so that it is applicable to a wide range of materials.

First, the accuracy of surface properties calculated with the thin-film approach depends strongly on the number of layers. To illustrate this point, the eigenvalues at $\vec{k} = \bar{\Gamma}(0,0)$ are plotted in Fig. 2 for Cu films one-, two-, three-, and five-layers thick, respectively. Abrupt termination potentials constructed with the bulk Cu Chodorow potential[12] were used for these four films as we wish to introduce the effects of surface potentials separately.

For a thin film, there is no Bloch vector k_z perpendicular to the film. Despite this the levels do resemble closely bulk bands if one arbitrarily plots the film eigenvalues at equal intervals in the z direction as is done in Fig. 2 for $\bar{\Gamma}(0,0)$. A one-layer thick film has only 6 eigenvalues for each $\vec{k} = (k_x, k_y)$ corresponding to the s and d valence states. A two-layer film has 12 states at each $\vec{k}$ as there are now two Cu atoms per unit cell. An n-layer film has $6n$ eigenvalues for each $\vec{k}$:

i.e., an n-layer film is plotted in Fig. 2 as 6 bands with n points per band. For an infinitely thick film, the 6 bands of n discrete states would become bulk bands where k_z is a real quantum number. For example, at $\bar{\Gamma}(0,0)$, the eigenvalues for a very thick film would become the bulk bands from $\Gamma(0,0,0)$ to $X(0,0,1)$ and contain approximately 10^{23} discrete states.

In a previous publication[2] we showed in detail that the eigenvalues for a five-layer Cu film are within 0.02 Ry of the corresponding bulk band states. Thus the one- and two-layer eigenvalues in Fig. 2 do not reproduce the bulk band shape whereas a five-layer film does. Another limitation of one-, two-, and three-layer films is that the two surfaces of the film are too close together for surface states to develop. Surface states are labeled only for the five-layer film. The probability distribution from layer to layer for the lower-energy surface state in Fig. 2 is 0.36, 0.12, 0.04, 0.12, and 0.36. The distribution of the higher-energy state is 0.30, 0.15, 0.10, 0.15, and 0.30.

One limitation of the five-layer film is that there is no band edge with which to directly determine the splitting of the surface state. Within LCMTO, this deficiency is overcome by performing a bulk calculation with the identical basis set. One then finds that the surface state ($E = -0.87$ Ry) in Cu at $\bar{\Gamma}(0,0)$ is split from the bulk band edge by ~ 0.007 Ry. However, such an estimate of the splitting can be in error depending on how strongly the surface states associated with the film faces overlap.

Next we wish to investigate the dependence of the thin-film results on the potential at the surface. A 20-layer film is chosen so that surface-state energies relative to band edge can be determined directly and so that the surface states on different surfaces do not overlap. We have chosen a Ni film here although similar results are obtained for Cu. The calculation is carried out at $\bar{\Gamma}(0,0)$ where symmetry reduces the Hamiltonian matrix to a manageable size.

Two different surface potentials were used. In the first case a bulk potential is placed on 18 layers and a surface potential (as defined in Sec. III) is placed on the two layers at one surface. The surface potentials on this face differ from bulk potentials and each other in that they are constructed with different number of nearest neighbors. The other surface is abruptly terminated. The $\Delta_1(s,z_2)$ symmetry states (SS) are plotted in Fig. 3 (states connected by solid line). SS at -0.873 Ry is the surface state localized at the surface potential face whereas CSS at -0.892 Ry refers to the state at the Cambridge-type abrupt termination potential face. This 0.02-Ry difference between SS and CSS is directly attributable to how the surface is terminated. The band edge is at -0.900 Ry. LEED[11] type calculations with a planar abrupt termination give a surface state ~ 0.01 Ry above

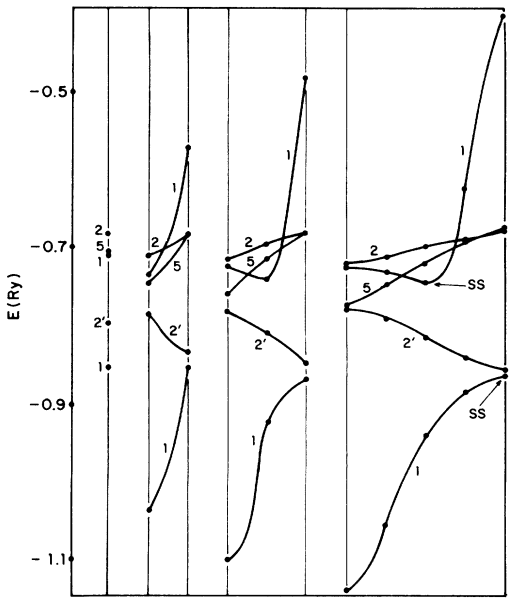

FIG. 2. Eigenvalues at $\bar{\Gamma}(0,0)$ for a Cu thin film one-, two-, three-, and five-layers thick, respectively. Solid line is drawn through states of a given symmetry type (SS).

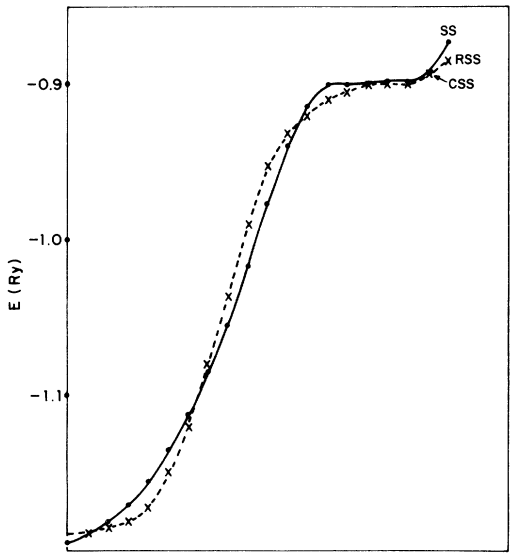

FIG. 3. Eigenstates (Δ_1 symmetry) at $\bar{\Gamma}(0,0)$ for (a) 20-layer film with two layers having surface potentials (see text) and (b) 20-layer film with one layer relaxed so that bond length is reduced by 3.2%. Surface state associated with corrugated Cambridge potential surface is CSS. Surface state with relaxed surface is RSS.

the band edge which agrees closely with CSS which is 0.008 Ry above the band edge.

In the second calculation only one surface was allowed to relax inwards such that the bond length between atoms in the top two layers is reduced by 3.22%. A new surface potential is calculated for the layers on this face. The other surface remains abruptly terminated with a bulk potential. The 20 Δ symmetry states (connected by dashes) are plotted in Fig. 3. CSS still occurs at -0.892 Ry, but SS has shifted by 0.011 Ry to -0.884 Ry and is labeled RSS for relaxed surface state. Thus for Ni, the surface states are very sensitive to the particular choice of surface potential. In a recent paper we have shown that the choice of surface potential is even more important in W and Mo.[7]

In the previously discussed calculations, the basis set consisted of nine *spd* decaying MTO's with $\kappa^2 = -0.25$ Ry. However, with LCMTO, oscillating MTO's with $\kappa^2 > 0$ can be used if we choose the hypothetical solid composed of thin films separated by several empty layers. We will make a comparison of the two approaches for a five-layer Ni film with a Cambridge-type abrupt termination potential. For the hypothetical solid the films will be separated by three empty layers thus giving a eight-layer unit cell.

In Fig. 4, the eigenvalue at $\bar{\Gamma}(0,0)$ of a five-layer film are connected by dashes. We choose $\kappa^2 = -0.25$ Ry to define the MTO basis set. The solid lines represent the corresponding bulk energy bands from $\Gamma(0,0,0)$ to $X(0,0,1)$. For a very thick film the two sets of states would become identical. However, even for five layers the energy difference between the bulk states and film states is less than 0.03 Ry. Also, the surface state at the top of the lower Δ_1 symmetry band is at -0.892 Ry in Fig. 3 and LEED calculations.[11]

In Fig. 5 we plot the eigenvalues at $\kappa^2 = (0,0,0)$ for a hypothetical solid of five-layer Ni films each separated by three empty layers from neighboring films. The basis set consisted of extended or oscillating MTO's with $\kappa^2 = 0.5$ Ry. We see that the agreement between thin-film and bulk states is much poorer than that for the localized basis set in Fig. 4. The surface state now occurs at -0.84 Ry, which is an error of 0.05 Ry. Thus a thicker film is required for a plane-wave type MTO basis set.

A basis set consisting of only nine *spd* MTO's ($\kappa^2 < 0$) as used in our thin-film calculations contains limited variational freedom. Such a basis set appears adequate for materials such as Ni and Cu because they are close-packed metals and surface effects are small. However, in materials such as W and Mo, surface effects cause large changes in energy (~ 0.1 Ry). It would appear necessary to allow for greater variational freedom in the basis set. The above results for a $\kappa^2 > 0$ MTO basis set indicate that it will be possible to mix MTO's with $\kappa^2 > 0$ and $\kappa^2 < 0$ as is done successfully in bulk solids.[5,8] Such a mixed basis set has recently been used to calculate electronic spectra in excellent agreement with experiment for CO molecules on Ni.[13] The enlarged basis set was necessary to represent the molecular levels. We believe this mixed basis set will be applicable to films of covalent materials such as Si and MoS_2.

One of the advantages of the thin-film approach is that chemisorption can be treated rather easily. However, the requirements of film thickness are different than for studying the surface states of a clean surface. In Fig. 6, we compare the effect of chemisorption of electronegative O and electropositive Na on a five-layer Ni(001) film at $\vec{\kappa} = \bar{\Gamma}(0,0)$. The surface structure is $c(1\times 1)$ with the atoms chemisorbed in the fourfold hollow sites. The O on Ni calculations were carried out for

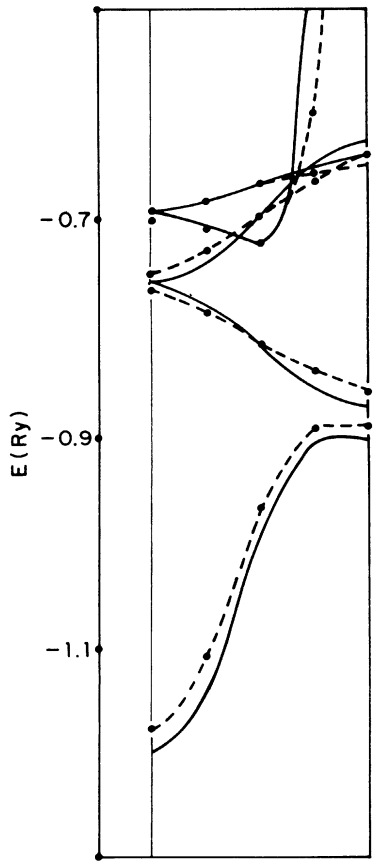

FIG. 4. Comparison of eigenstates at $\bar{\Gamma}(0,0)$ of a five-layer Ni film with those of corresponding bulk state (solid line). The same MTO parameters are used in both calculations. Dashed lines connect thin-film states of a given symmetry.

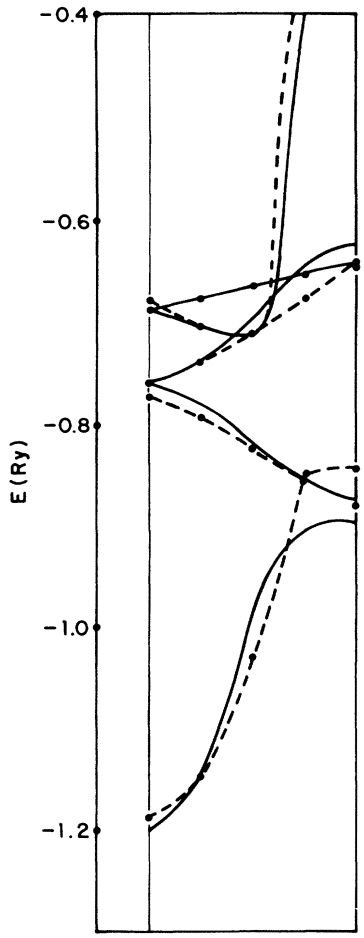

FIG. 5. Eigenstates at $\Gamma(0,0,0)$ for periodic Ni thin film (five-layer films separated by three empty layers). Solid line represents bulk bands. Dashed lines connect thin-film states.

Ni–O distances of 1.13 and 1.50 Å. The Na on Ni calculations were carried out for Na–Ni distances of 2.87 and 1.76 Å. In all four cases the effect of the adatoms is to cause strongly localized surface states to form which are represented by an × in Fig. 6. The O-p derived states are marked by a p. Note that the bulklike states are changed little by chemisorption and only the surface-state energies are shifted by the chemisorption. The shifts are large (~0.1 Ry). Electronegative O causes states to shift upwards and electropositive Na causes downward shifts. It appears that a five-layer film is a very adequate model because the chemisorption effects are large. These chemisorption results have been discussed previously.[4]

The above considerations deserve summation. First, it appears that localized MTO functions describe accurately the electronic properties of transition metals. Application of LCMTO to covalently bonded systems will undoubtedly require

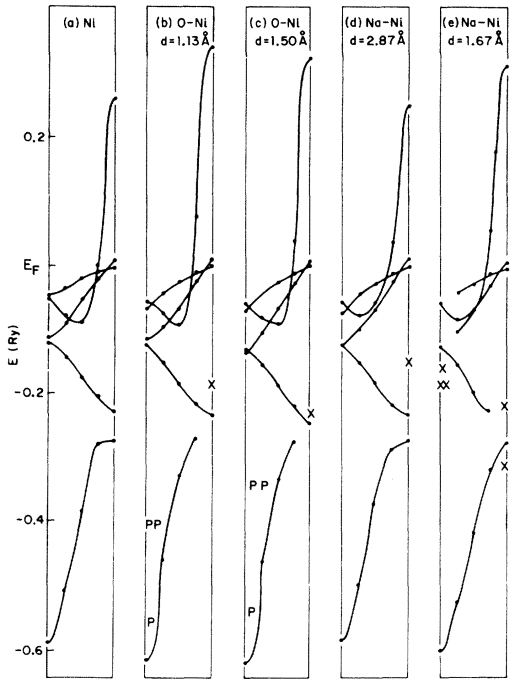

FIG. 6. Energy states of (a) five-layer Ni(001) thin film and the effect on these thin-film states of (b) O overlayer at $d=0.90$ Å, (c) O overlayer at $d=1.50$ Å, (d) Na overlayer at $d=2.87$ Å, and (e) Na overlayer at $d=1.76$ Å. O $2p$ states are represented by a p, while induced surface states are represented by an ×.

a larger basis set. The most logical approach to improving the LCMTO basis set is to mix localized short-range and oscillating long-range MTO's. This approach is excellent for bulk materials such as Si and MoS_2 and should be accurate for their surfaces also. For metals, the use of localized MTO's appears adequate and allows one to use thinner films than might be required with an oscillating long-range MTO- or OPW-type basis set. The thicker film is required so that the long-range oscillating tails can cancel in vacuum. A considerable monetary savings results as the cost of a calculation is proportional to N^3 where N is the number of layers.

Our calculations on Cu films indicate that films only one- or two-layers thick are poor representations of the bulk solid and its surface. In Fig. 2 the size of the Cu s-d band gap changed dramatically with layer thickness. One would expect band-gap surface states to be inaccurate if the film is too thin.

V. MOLECULAR CALCULATIONS

The LCMTO formalism is also applicable to molecules. However, κ^2 in Eq. (2) must be restricted to negative values. Such a calculation was

performed for a N_2 molecule. The potential was formed by overlapping atomic charge densities[9] and using Slater exchange.

The ionization potential (IP) of a molecular level is equal to the difference in total energy of the initial state and the ion. Such calculations are expensive to perform. Slater and Wood[14] have devised the transition-state approximation whereby the IP is equal to the one-electron energy of the molecular orbital with $\frac{1}{2}$ an electron removed. This procedure is economical and accurate for use with free-electron exchange potentials and $\alpha = 0.7$.

These transition-state calculations[15,16] have shown that the difference between the one-electron eigenvalues and the corresponding IP's is nearly a constant. Also, the IP calculated for a potential with $\alpha = 0.7$ is approximately equal to the eigenvalues calculated with an $\alpha = 1.0$ potential. Thus we will simply approximate the IP's of N_2 by their one-electron eigenvalues since $\alpha = 1.0$ is used. In this calculation, we are primarily concerned with obtaining the correct ordering and interlevel spacing.

There are numerous calculations with which to compare. In Fig. 7 we compare our calculated ionization potential energies with those of experiment,[17] Hartree-Fock,[18] the scattered wave (SW) method,[19] and the discrete variational method[20] (DVM). Our ionization potentials are taken as the one-electron energies with no relaxation or other final-states effects taken into account. The LCMTO basis set consisted of only 4 MTO's per N atom. An incorrect spacing of the $3\sigma_g$ and $1\pi_u$ resulted as seen in Fig. 6. The Hartree-Fock calculation obtains an incorrect ordering of these two levels (Fig. 6) although a correct ordering is obtained if configuration interaction is included.[21]

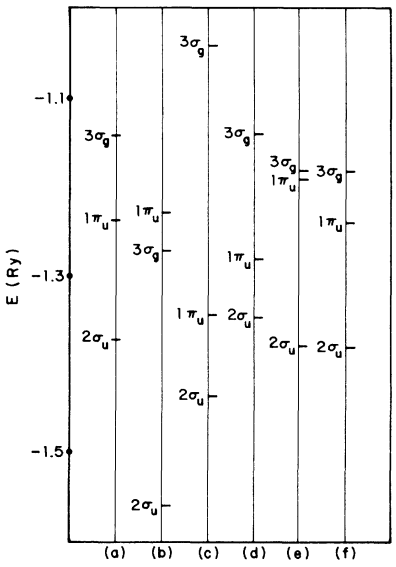

FIG. 7. Ionization potentials of a N_2 molecule. (a) experimental ionization potentials,[14] (b) Hartree-Fock,[15] (c) SW method,[16] (d) DVM,[17] (e) LCMTO using 4 MTO's, (f) mixed MTO's plus GTO's.

The major deficiency of the LCMTO method for molecules is that the MTO's decay too rapidly, e^{-kr}/r. This deficiency can be overcome by mixing a few Gaussian-type orbitals (GTO) or Slater-type orbitals with the MTO basis set since these orbitals have appropriate long-range tails. The secular equation now reads

$$\langle \psi_{\mathrm{GTO}} + \psi_{\mathrm{MTO}} | -\nabla^2 + V(r) - E | \psi_{\mathrm{MTO}} + \psi_{\mathrm{GTO}} \rangle = 0.$$

Implementation requires that GTO's be expanded in terms of spherical harmonics and radial numerical functions about one center. Such a calculation was performed for N_2 with a basis set of 4 MTO's and 3 GTO's per atom. The results in Fig. 7(f) compare favorably with experiment. We note that the SW method [Fig. 7(c)] overestimates the $3\sigma_g - 1\pi_u$ separation by ~0.20 Ry. The DVM method overestimated the $3\sigma_g - 1\pi_u$ splitting by ~0.1 Ry.

An alternative to mixing GTO's and MTO's could be to form a hypothetical solid of molecules. One could then mix long-range oscillating MTO's with the short-range decaying functions. This approach has been used to study chemisorption of CO molecules on a Ni surface.[13]

ACKNOWLEDGMENTS

I wish to thank Dr. H. S. Jarrett for many helpful discussions and a critical reading of the manuscript. I thank G. Alldredge for a reading of the manuscript.

APPENDIX A

In this section, Eq. (2) is derived using the definition of the muffin-tin orbital $\chi_L(E_1, \kappa_1, \vec{\gamma}_1)$ in Sec. II. In previous work,[4] we found that continuity of the logarithmic derivative at the muffin-tin sphere (5) requires

$$s_l(E,K) = S^2[J_l(\kappa)\varphi_l'(E) - J_l'(\kappa)\varphi_l(E)]_{r=s} = \int_0^s \varphi_l(E)(V_{\mathrm{MT}} - E + \kappa^2) J_l(\kappa) r^2 \, dr$$

and

$$c_l(E,\kappa) = -S^2[K_l(E)\varphi_l'(E) - K_l'(\kappa)\varphi_l(E)]_{r=s},$$

where the prime indicates the radial derivative. Contrary to previous work,[4] we will normalize φ_l so that $s_l(E,\kappa) = 1$ always.

A multicentered MTO Block function expanded about site Q is formed for parameters κ_1^2 and E_1 with $\vec{r}_1 = \vec{r} - \vec{q}_1$.

$$\psi^{\vec{k}}_{q_1 L_1}(\vec{r}_1) = \frac{1}{\sqrt{N}} \sum \exp(i\vec{k}\cdot\vec{R}n)\chi_{L_1}(r_1, \kappa_1, E_1)$$

$$= \frac{1}{\sqrt{N}} \left(\varphi_{q_1 L_1}\delta_{q_1, Q} + \sum_{L_3} J_{L_3}(r - Q) B_{QL_3, q_1 L_1} \right). \quad (3)$$

$B_{QL_3, q_1 L_1}$ is the Korringa-Kohn-Rostoker matrix.[4] Substitution of Eq. (3) yields

$$B_{QL_3, q_1 L_1} = C_{q_1 L_1}\delta_{q_1 Q, L_1 L_3} - \sum_{L''} 4\pi C_{L_1 L_3 L''} \kappa^{l_1 + l_3 - l''} \times \sum_R (1 - \delta_{Q - q_1, R}) e^{i\vec{k}\cdot\vec{R}} K_{L''}(q_1, -Q).$$

Application of the linear variational principle to $H - E$ yields the general matrix elements (let $l = q_1 L$):

$$\frac{1}{N}\langle \psi^{\vec{k}}_{q_1 L_1}(E_1, \kappa_1, \vec{r}_1) | H - E | \psi^{\vec{k}}_{q_2 L_2}(E_2, \kappa_2, \vec{r}_2) \rangle$$
$$= \langle \varphi_1 | \Delta V + E_2 - E | \varphi_2 \rangle \delta_{q_1, q_2}$$
$$+ \langle \varphi_1 | \kappa_2^2 - E_2 + V_{\mathrm{MT}} | J_1 \rangle T_{12}$$
$$+ \sum_4 \langle \varphi_1 | E_2 \delta_{l_4 = 0} + \Delta V - E | J_4 \rangle T_{42} + \mathrm{H.c.}$$
$$+ \sum_3 \sum_4 T_{13} \langle J_3 | V_{\mathrm{MT}} + \Delta V + \kappa_2^2 - E | J_4 \rangle T_{42}.$$

ΔV is the non-muffin-tin part of the potential.

[1] G. P. Alldredge and L. Kleinman, Phys. Rev. Lett. 28, 1264 (1972); Phys. Rev. B 10, 559 (1974).
[2] R. V. Kasowski, Phys. Rev. Lett. 33, 83 (1974); 33, 1147 (1974).
[3] M. Schluter, J. R. Chelikowsky, S. G. Louie, and M. L. Cohen, Bull. Am. Phys. Soc. 20, 324 (1975).
[4] O. K. Andersen and R. V. Kasowski, Phys. Rev. B 4, 1064 (1971); R. V. Kasowski and O. K. Andersen, Solid State Commun. 11, 799 (1972).
[5] R. V. Kasowski, Phys. Rev. B 8, 1378 (1973).
[6] E. Caruthers and L. Kleinman, Phys. Rev. Lett. 35, 738 (1975).
[7] R. V. Kasowski, Solid State Commun. 17, 179 (1975).
[8] R. V. Kasowski, Phys. Rev. Lett. 30, 1175 (1973).
[9] F. Herman and S. Skillman, *Atomic Structure Calculations* (Prentice-Hall, Englewood Cliffs, N. J., 1963).
[10] O. Jepsen, O. K. Andersen, and A. R. Mackintosh, Phys. Rev. B 12, 3084 (1975).
[11] F. Forstmann and V. Heine, Phys. Rev. Lett. 24, 1419 (1970).
[12] Chodorow potential is tabulated in G. A. Burdick, Phys. Rev. 129, 138 (1963).
[13] R. V. Kasowski (unpublished).
[14] J. C. Slater and J. H. Wood, Intern. J. Quantum Chem. 3, 45 (1971).
[15] D. E. Ellis (private communication).
[16] K. H. Johnson (private communication).
[17] K. Siegbahn, C. Nordling, C. Johansson, J. Hedman, P. F. Heden, K. Hamrin, U. Gelius, T. Bergmark, L. O. Werme, R. Manne, and Y. Baer, *ESCA Applied to Free Molecules* (North-Holland, Amsterdam, 1969).
[18] P. E. Cade, K. D. Sales, and A. C. Wahl, J. Chem. Phys. 44, 1973 (1966).
[19] B. Danese (unpublished).
[20] E. J. Baerends and P. Ros, Chem. Phys. 2, 52 (1973).
[21] G. Verhaegen, W. G. Richards, C. M. Moser, J. Chem. Phys. 47, 2595 (1967).